doi:10.1038/nature12623

Supplementary Table 1| Steady-state parameters for cleavage of 5-nitrobenzisoxazole by representative Kemp eliminases[a]

Catalyst	k_{cat} (s^{-1})	K_M (mM)	k_{cat}/K_M (M^{-1} s^{-1})	$(k_{cat}/K_M)/k_{AcO^-}$ [b]	k_{cat}/k_{uncat} [c]	Ref
34E4[d]	0.66	0.12	5.5×10^3	9.5×10^7	5.7×10^5	11
KE59[e]	nd	nd	160	2.8×10^6	nd	12
KE59.13[e,f]	9.5 ± 0.6	0.16 ± 0.02	5.9×10^4	1.0×10^9	8.2×10^6	14
HG3[g]	3.0 ± 0.1	2.4 ± 0.3	1.3×10^3	2.2×10^7	2.6×10^6	
HG3.3b[h]	14 ± 2	2.6 ±0.6	5.4×10^3	9.3×10^7	1.2×10^7	
HG3.7[g]	310 ± 130	8.3 ± 3.2	3.7×10^4	6.5×10^8	2.7×10^8	
HG3.14[g]	490 ± 100	7.0 ± 2.0	7.0×10^4	1.2×10^9	4.2×10^8	
HG3.17[g]	700 ± 60	3.0 ± 0.3	2.3×10^5	4.0×10^9	6.0×10^8	

[a] For comparison, the TIM-catalyzed conversion of dihydroxyacetone phosphate to glyceraldehyde-3-phosphate has been assayed at 30°C in 100 mM triethanolamine-HCl buffer pH 7.27, giving the steady-state parameters k_{cat} = 430 s^{-1}, K_M = 0.97 mM and $k_{cat}/K_M = 4.4 \times 10^5$ M^{-1} s^{-1} (ref. 15). The k_{cat}/k_{uncat} value was reported to be 7.2×10^8 but because the published k_{uncat} value [Hall, A. & Knowles, J. R., *Biochemistry* **14**, 4348-4352, (1975)] overestimates the uncatalyzed rate of DHAP deprotonation (k_{HO^-} = 0.56 M^{-1} s^{-1}, ref. 10), $k_{cat}/(k_{HO^-}[HO^-]) = 4.1 \times 10^9$ gives a more realistic estimate of the enzyme's catalytic prowess.

[b] The advantage over acetate in solution was calculated using the second-order rate constant for the acetate-promoted reaction measured at pH 7 and 27°C in the presence of 10% MeOH ($k_{AcO^-} = 5.77 \times 10^{-5}$ M^{-1} s^{-1}). For comparison, the rate constant for hydroxide-catalyzed deprotonation of 5-nitrobenzisoxazole is 15 M^{-1} s^{-1} (ref. 9).

[c] Rate accelerations for the Kemp eliminases were calculated based on the rate constant for the uncatalyzed reaction determined in ref. 12 ($k_{uncat} = 1.16 \times 10^{-6}$ s^{-1}).

[d] Assay conditions: 20°C, 40 mM sodium phosphate pH 7.4, 100 mM NaCl.

[e] Assay conditions: 27°C, 25 mM HEPES pH 7.25, 100 mM NaCl, 1.5 % MeCN, 1.25 % glycerol.

[f] Although 5-nitrobenzisoxazole was used during optimization of KE59, the best substrate for KE59.13 was found to be 5,7-dichlorobenzisoxazole: k_{cat} = 21 s^{-1}, K_M = 0.037 mM and $k_{cat}/K_M = 5.7 \times 10^5$ M^{-1} s^{-1}. The rate acceleration (k_{cat}/k_{uncat}) for this substrate is 2.5×10^7 (ref. 14).

[g] Assay conditions: 27°C, 50 mM sodium phosphate buffer pH 7.0, 100 mM NaCl, 10 % MeOH. Errors correspond to standard deviations determined from at least two independent measurements. For HG3.17, six measurements on three independent protein batches were made. For comparison, the k_{cat} and K_m values for the starting HG3 design were reported to be 1.7 ± 0.1 s^{-1} and 2.4 ± 0.2 mM in the same buffer but containing 2% acetonitrile instead of 10% methanol (ref. 3).

[h] Assay conditions: 27°C, 50 mM sodium phosphate buffer pH 7.0, 100 mM NaCl, 2 % MeCN

Supplementary Table 2| Crystallographic data and refinement statistics

	HG3.17-E47N/N300D
Data collection	
Space group	$P2_12_12_1$
Cell dimensions	
a, *b*, *c* (Å)	76.08, 77.95, 98.28
α, β, γ (°)	90.00, 90.00, 90.00
Resolution (Å)	28.3-1.09 (1.13-1.09)
R_{meas} (%)	4.1 (45.6)
$I / \sigma I$	32.1(4.9)
CC 1/2 (%)	100.0 (92.2)
Completeness (%)	93.1(57.0)
Redundancy	12.2(7.3)
Refinement	
Resolution (Å)	28.3-1.09
No. reflections	225746
R_{work} / R_{free} (%)	12.4 / 14.5
No. atoms	
All	15025
Non-hydrogen	8042
Protein[a]	14068
Ligand[a]	48
Solvent	909
B-factors	
All	13.78
Non-hydrogen	13.58
Protein[a]	12.73
Ligand[a]	8.71
Solvent	30.18
R.m.s. deviations	
Bond lengths (Å)	0.015
Bond angles (°)	1.308

[a] Including hydrogen atoms.

*Highest-resolution shell is shown in parentheses.

Supplementary Table 3| Cloning primers

Name	Sequence 5'- 3'
T7 Terminator	AAG ACC CGT TTA GAG GCC CCA A
T7_Alternative	GAT CCC GCG AAA TTA ATA CGA CTC ACT ATA GG
HG3_middle	TCC GCG CGT GGG ATG TTG
HG3_M172	TCC AAA CGC TAA GCT GTA CAT ANN KGA TTA CAA CCT GGA CTC TGC G
HG3_M172_revcomp	ATG TAC AGC TTA GCG TTT GGA TC
HG3_E131	CGC GTG GGA TGT TGT GGG TNN KGC ATT CAA CGA GGA CGG C
HG3_E131_revcomp	CCC ACA ACA TCC CAC GCG
HG3_S89_Q90	GTG GCA TGC TGG TTT GGC ATN DTN DTC TGC CGT CTT GGG TGT CTT C
HG3_S89_Q90_revcomp	TGC CAA ACC AGC ATG CCA C
HG3_T265	GTG CAG TCT TGT GTG GGC ATA NNK GTA TTT GGT GTT GCC GAT CCT G
HG3_T265_revcomp	ATG CCC ACA CAA GAC TGC AC
HG3_R124_A125	GAT GAC CCG TTA TAA AGG CAA AAT TND TND TTG GGA TGT TGT GGG CGA AG
HG3_R124_A125_revcomp	ATT TTG CCT TTA TAA CGG GTC ATC
HG3_V6_I10	GGC AGA AGC GGC TCA ATC TND TGA CCA ACT TND TAA AGC TCG TGG TAA AGT GTA TTT C
HG3_V6_I10_revcomp	GAT TGA GCC GCT TCT GCC
HG3_L236_M237	GCA CTC CGG AGG TTA GCA TTN DTN DTC TGG ATG TAG CGG GCG C
HG3_L236_M237_revcomp	ATG CTA ACC TCC GGA GTG C
HG3_K50	GGT TTG GCC AGA GAA CTC CAT GND TTG GGA CGC GAC CGA GC
HG3_K50_revcomp	ATG GAG TTC TCT GGC CAA ACC
HG3_M84	TAA GCT GAT CGG CGG TGG TND TCT GGT TTG GCA CAG CCA G
HG3_M84_revcomp	CCA CCG CCG ATC AGC TTA
HG3_pMG209_NcoI	ATA TAC CCA TGG CAG AAG CGG CTC AAT CC
HG3_pMG209_XhoI	ATG GTG CTC GAG ACC ACG ACC CTC GAT GCT GC
HG3_pET11_NdeI	GAT ATA CAT ATG GCA GAA GCG GCT CAA TCC
HG3_pET11_BamHI	GCA GCC GGA TCC CTA ATG GTG GTG GTG ATG GTG ACC ACG ACC CTC G
HG3.14_S89_H90_NDT	GGT TGT CTG GTC TGG CAC NDT NDT CTG CCG TCT TGG GTG TCT TC
HG3.14_S89_H90_VHG	GGT TGT CTG GTC TGG CAC VHG VHG CTG CCG TCT TGG GTG TCT TC
HG3.14_S89_H90_revcomp	GTG CCA GAC CAG ACA ACC
HG3.14_E46_N47_VAG	GCA GAT TTC GGT ATG GTT TGG CCA VAG VAG TCC ATG CAA TGG GAC GCG ACC
HG3.14_E46_N47_NNC	GCA GAT TTC GGT ATG GTT TGG CCA NNC NNC TCC ATG CAA TGG GAC GCG ACC
HG3.14_E46_N47_revcomp	AAC CAT ACC GAA ATC TGC
HG3.14_M237_NDT	GCA CTC CGG AGG TTA GCA TCT TGN DTC TGG ATG TAG CGG GCG CAA GC
HG3.14_M237_VHG	GCA CTC CGG AGG TTA GCA TCT TGV HGC TGG ATG TAG CGG GCG CAA GC
HG3.14_M237_revcomp	TGC TAA CCT CCG GAG TGC
HG3.14_F267_NDT	GCA GTC TTG TGT GGG CAT TAC CGT AND TGG TGT TGC CGA TCC TGA TTC TTG G
HG3.14_F267_VHG	GCA GTC TTG TGT GGG CAT TAC CGT AVH GGG TGT TGC CGA TCC TGA TTC TTG G
HG3.14_F267_revcomp	ATG CCC ACA CAA GAC TGC
HG3.14_W87_H88_NNK-NNT	GCT GAT CGG CGC TGG TTG TCT GGT CNN KNN TTC CCA TCT GCC GTC TTG GGT GTC TTC C
HG3.14_W87_H88_revcomp	CCA GAC AAC CAG CGC CGA TCA GC
HG3.14_W275_R276_NNK-NNT	GGT GTT GCC GAT CCT GAT TCT NNK NNT GCG TCC AGT ACC CCG CTG C
HG3.14_W275_R276_revcomp	AAT CAG GAT CGG CAA CAC C
HG3.14_T265_NNT	GTG CAG TCT TGT GTG GGC ATT NNT GTA TTT GGT GTT GCC GAT CC
HG3.14_T265_revcomp	ATG CCC ACA CAA GAC TGC AC
HG3.14_T125_NNK	CGT TAT AAA GGC AAA ATC CGC NNK TGG GAT GTT GTG GGC GAA GC
HG3.14_T125_revcomp	GCG GAT TTT GCC TTT ATA ACG
HG3.14_88-90_SMT-MRT-YAC	GCT GGT TGT CTG GTC TGG SMT MRT YAC CTG CCG TCT TGG GTG TCT TCC
HG3.14_88-90_SMT-MRT-TYT	GCT GGT TGT CTG GTC TGG SMT MRT TYT CTG CCG TCT TGG GTG TCT TCC
HG3.17_D127N	GAT GAC CCG TTA TAA AGG CAA AAT CCG CAC GTG GAA TGT TGT GGG CGA AGC ATT C
HG3.17_D127A	GAT GAC CCG TTA TAA AGG CAA AAT CCG CAC GTG GGC TGT TGT GGG CGA AGC ATT C
HG3.17_Q50A	GGT TTG GCC AGA GGA GTC CAT GGC TTG GGA CGC GAC CGA GC
HG3.17_Q50_revcomp	ATG GAC TCC TCT GGC CAA ACC
HG3.17_N300D	GCT TAC AAC GCT ATC GTT CAG GAC TTG CAA CAG GGC AGC ATC GAG G
HG3.17_N300_revcomp	CTG AAC GAT AGC GTT GTA AGC

Supplementary Table 4a | Construction and activity of focused HG3 libraries[a]

Round	Library	Design category	Codon	No. of clones screened	Improvement (% of precursor)	Best sequence
1b	Val6/Ile10	HS	NDT	430	140	V6I_I10I
	Lys50/Met84	R	NDT	430	600	K50H_M84C
	Ser89/Gln90	HS	NDT	430	230	S89R_Q90D
	Arg124/Ala125	HS	NDT	430	180	R124R_A125N
	Glu131	HS	NNK	96	150	E131Q
	Met172	HS	NNK	96	500	M172I
	Leu236/Met237	R	NDT	430	125	L236L_M237C
	Thr265	R	NNK	96	100	T265T
15	Ser89/His90	HS/ET	NDT+VHG	1152	200	S89N_H90F
	Glu46/Asn47	ET	VAG+NNC	1152	140	E46_N47E
	Met237/Phe267	ET	NDT+VHG	1152	130	M237_F267M
	Trp87/His88	ET	NNK/NNT	1152	130	W87_H88D
	Thr125/T265	HS	NNK/NNT	1152	100	T125_T265
	Met172	HS	NNK	96	100	M172
	Trp275/Arg276	ET	NNK/NNT	1152	160	W275A_R276F

[a] (HS = based on hot spots, R = based on visual inspection of the design crystal structure, ET = close to entry tunnel).

Supplementary Table 4b| Iterative combination of beneficial mutations

Round	Clone No.	Constant mutations	Variable mutations	Improvement (% of precursor)	Best sequence
3b	1a		S89R/Q90D	250	
	1b	K50C/M84L/M172I	S89R/Q90D/A125N	170	
	1c		S89R/Q90D/A125N/V6I	450	S89R/Q90D/A125N/V6I
	2a		S89R/Q90D	500	
	2b	K50H/M84C/M172I	S89R/Q90D/A125N	500	S89R/Q90D/A125N
	2c		S89R/Q90D/A125N/V6I	450	
	3a		S89R/Q90D	300	
	3b	K50H/M84C	S89R/Q90D/A125N	700	
	3c		S89R/Q90D/A125N/V6I	750	S89R/Q90D/A125N/V6I

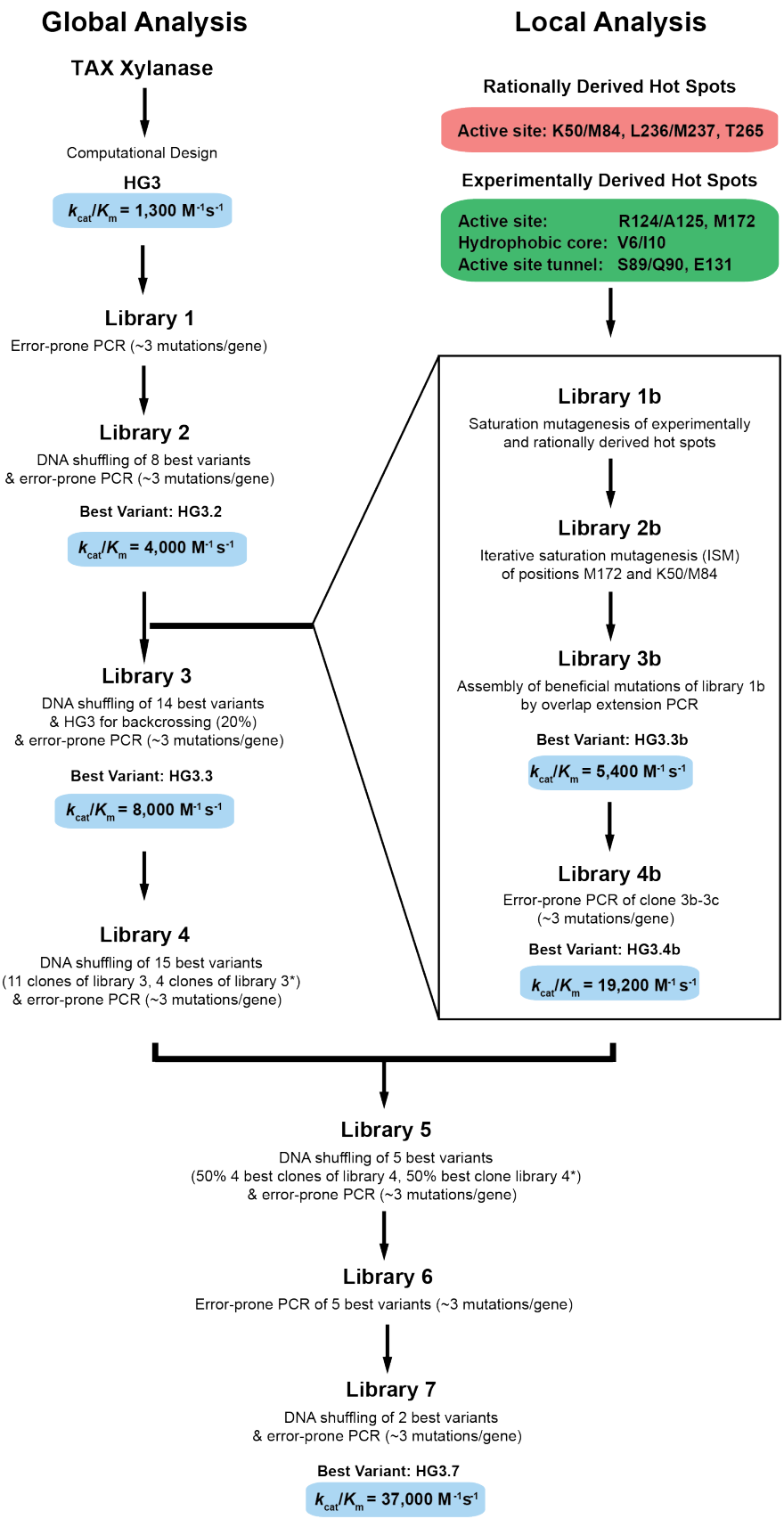

Supplementary Figure 1a | Evolutionary optimization of HG3 (Rounds 1-7)

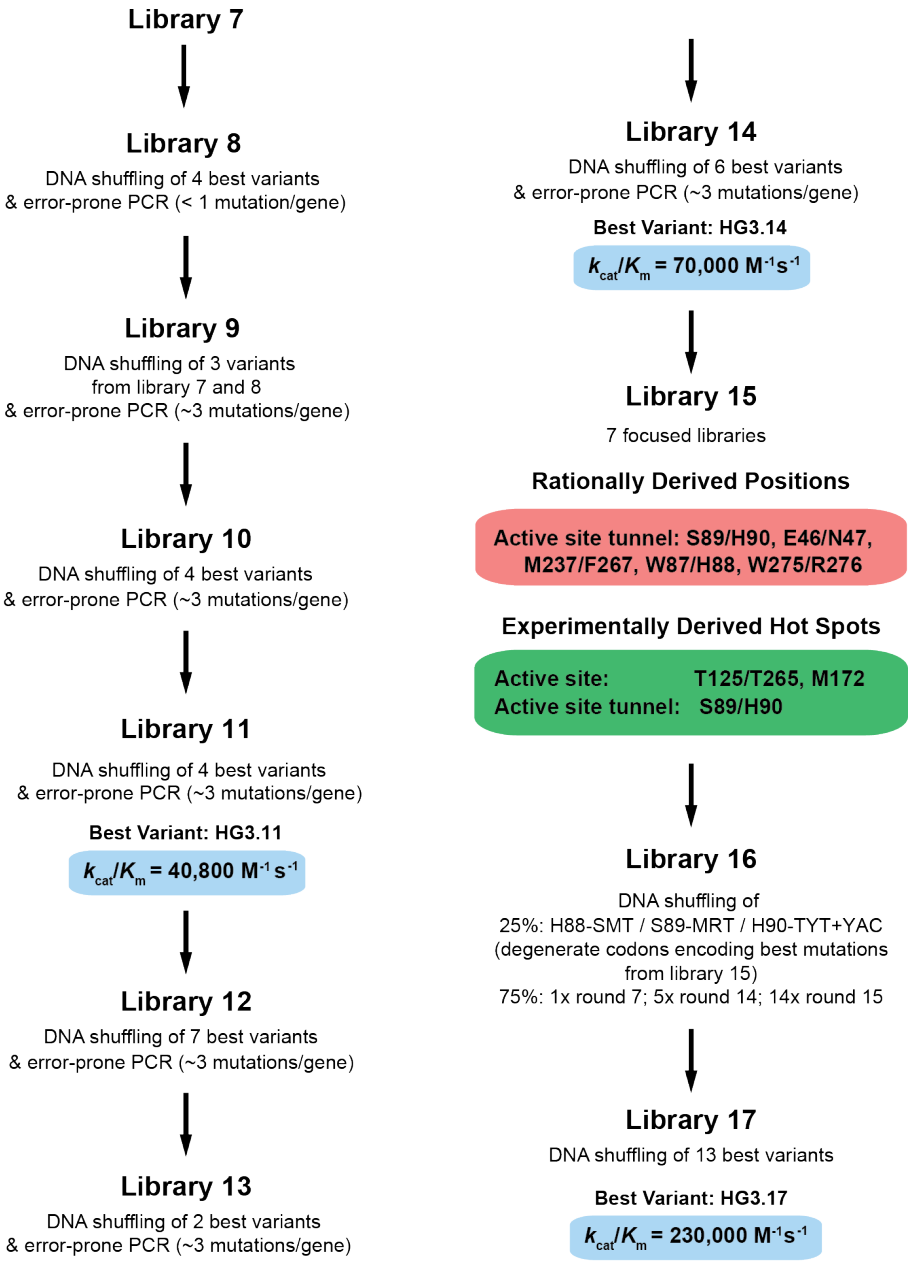

Supplementary Figure 1b | Evolutionary optimization of HG3 (Rounds 8 – 17)

HG3:

MAEAAQSVDQLIKARGKVYFGVATDQNRLTTGKNAAIIQADFGMVWPENSMKWDATEPSQGNFNFAGA
DYLVNWAQQNGKLIGGGMLVWHSQLPSWVSSITDKNTLTNVMKNHITTLMTRYKGKIRAWDVVGEAFN
EDGSLRQTVFLNVIGEDYIPIAFQTARAADPNAKLYIMDYNLDSASYPKTQAIVNRVKQWRAAGVPID
GIGSQTHLSAGQGAGVLQALPLLASAGTPEVSILMLDVAGASPTDYVNVVNACLNVQSCVGITVFGVA
DPDSWRASTTPLLFDGNFNPKPAYNAIVQDLQQGSIEGRGHHHHHH

HG3.3b: V6I, K50H, M84C, S89R, Q90D, A125N

MAEAAQSIDQLIKARGKVYFGVATDQNRLTTGKNAAIIQADFGMVWPENSMHWDATEPSQGNFNFAGA
DYLVNWAQQNGKLIGGGCLVWHRDLPSWVSSITDKNTLTNVMKNHITTLMTRYKGKIRNWDVVGEAFN
EDGSLRQTVFLNVIGEDYIPIAFQTARAADPNAKLYIMDYNLDSASYPKTQAIVNRVKQWRAAGVPID
GIGSQTHLSAGQGAGVLQALPLLASAGTPEVSILMLDVAGASPTDYVNVVNACLNVQSCVGITVFGVA
DPDSWRASTTPLLFDGNFNPKPAYNAIVQDLQQGSIEGRGHHHHHH

HG3.7: V6I, Q37K, K50Q, M84C, S89R, Q90H, A125N

MAEAAQSIDQLIKARGKVYFGVATDQNRLTTGKNAAIIKADFGMVWPENSMQWDATEPSQGNFNFAGA
DYLVNWAQQNGKLIGGGCLVWHRHLPSWVSSITDKNTLTNVMKNHITTLMTRYKGKIRNWDVVGEAFN
EDGSLRQTVFLNVIGEDYIPIAFQTARAADPNAKLYIMDYNLDSASYPKTQAIVNRVKQWRAAGVPID
GIGSQTHLSAGQGAGVLQALPLLASAGTPEVSILMLDVAGASPTDYVNVVNACLNVQSCVGITVFGVA
DPDSWRASTTPLLFDGNFNPKPAYNAIVQDLQQGSIEGRGHHHHHH

HG3.14: V6I, Q37K, K50Q, G82A, M84C, Q90H, T105I, A125T, T142N, T208M, T279S, D300N

MAEAAQSIDQLIKARGKVYFGVATDQNRLTTGKNAAIIKADFGMVWPENSMQWDATEPSQGNFNFAGA
DYLVNWAQQNGKLIGAGCLVWHSHLPSWVSSITDKNTLINVMKNHITTLMTRYKGKIRTWDVVGEAFN
EDGSLRQNVFLNVIGEDYIPIAFQTARAADPNAKLYIMDYNLDSASYPKTQAIVNRVKQWRAAGVPID
GIGSQMHLSAGQGAGVLQALPLLASAGTPEVSILMLDVAGASPTDYVNVVNACLNVQSCVGITVFGVA
DPDSWRASSTPLLFDGNFNPKPAYNAIVQNLQQGSIEGRGHHHHHH

HG3.17: V6I, Q37K, N47E, K50Q, G82A, M84C, S89N, Q90F, T105I, A125T, T142N, T208M, F267M, W275A, R276F, T279S, D300N

MAEAAQSIDQLIKARGKVYFGVATDQNRLTTGKNAAIIKADFGMVWPEESMQWDATEPSQGNFNFAGA
DYLVNWAQQNGKLIGAGCLVWHNFLPSWVSSITDKNTLINVMKNHITTLMTRYKGKIRTWDVVGEAFN
EDGSLRQNVFLNVIGEDYIPIAFQTARAADPNAKLYIMDYNLDSASYPKTQAIVNRVKQWRAAGVPID
GIGSQMHLSAGQGAGVLQALPLLASAGTPEVSILMLDVAGASPTDYVNVVNACLNVQSCVGITVMGVA
DPDSAFASSTPLLFDGNFNPKPAYNAIVQNLQQGSIEGRGHHHHHH

Supplementary Figure 2 | Amino acid sequences of representative HG3 variants. Sequence numbering of HG3 is based on the X-ray structure of HG2 (PDB code 3NYQ, chain A), the first two residues of which are not resolved. The HG3 sequence is used as reference for the highlighted mutations (orange = residue was computationally designed into the TAX xylanase scaffold 1GOR, green = residue was mutated once in the course of evolution, cyan = residue was mutated twice in the course of evolution, magenta = residue was mutated three times in the course of evolution).

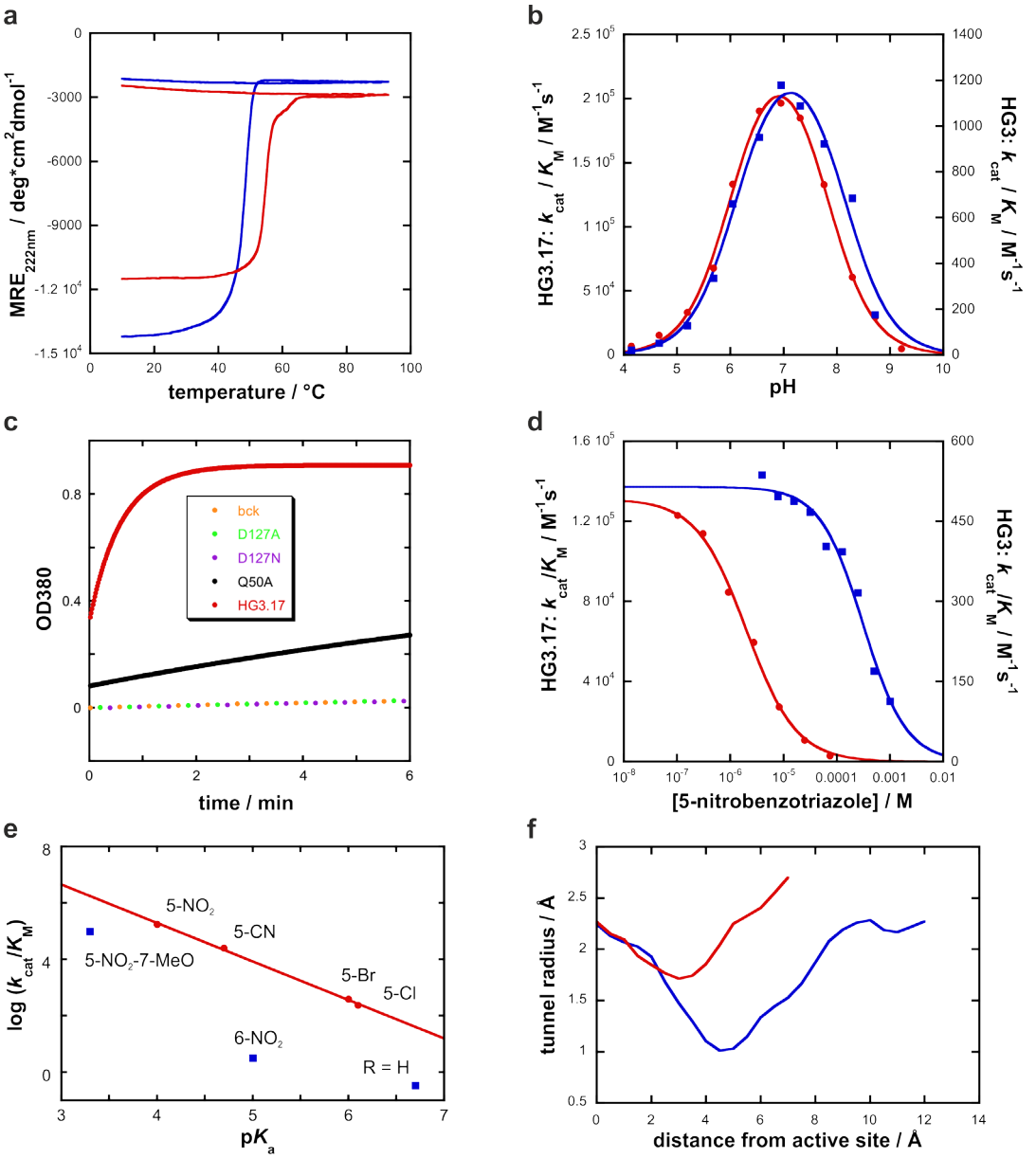

Supplementary Figure 3 | Biochemical characterization of HG3.17 and comparison with HG3. (a) Thermal denaturation of HG3.17 (red) and HG3 (blue). (b) pH-rate profiles for HG3.17 (red) and HG3 (blue). (c) Cleavage of 50 µM 5-nitrobenzisoxazole by HG3.17 variants (background buffer reaction: orange; D127A: green ([HG3.17 D127A] = 10 µM); D127N: purple ([HG3.17 D127N] = 10 µM); Q50A: black ([HG3.17 Q50A] = 100 nM); HG3.17 (wt): red ([HG3.17] = 100 nM)). For HG3.17 and HG3.17 Q50A, data points are shown at 1 s intervals. For the other measurements, points are only shown at 33 s intervals for clarity. (d) K_i determination of the transition state analog 6-nitrobenzotriazole with HG3.17 (red, K_i = 2 µM) and HG3 (blue, K_i = 310 µM) at pH 6.0. (e) Brønsted plot for cleavage of substituted benzisoxazoles reveals the discriminating nature of HG3.17. The β value for the 5-substituted substrates is -1.36. (f) The length and width of the substrate entry tunnel of HG3.17 (red) and HG2 (= HG3-T265S, blue) were measured with the PyMOL plugin Caver 3.0 (ref. 47). Since the structure of HG2 was solved without hydrogen atoms, these were added in PyMOL before performing the calculation.

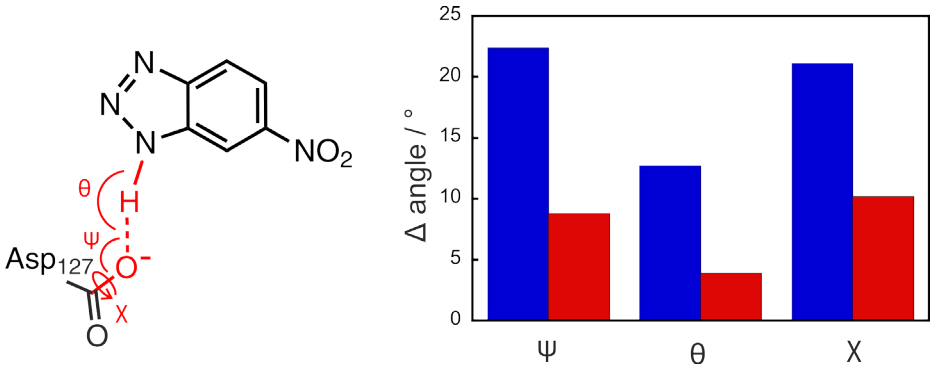

Supplementary Figure 4 | Evolutionary optimization of the angles characterizing the hydrogen-bonding interaction between Asp127 and the transition state analog. Values are given as the difference between the optimal angles calculated for hydrogen bonding interactions between acetamide dimers[47] (ψ = 112.3°, θ = 159.4°, X = 177.5°) and the measured values for the hydrogen bond between 6-nitrobenzotriazole and the catalytic base Asp127 in HG2 (blue, ψ = 134.7°, θ = 172.1°, X = 156.4°) and HG3.17 (red, ψ = 121.1°, θ = 155.5°, X = 167.3°). For the HG2 (i.e. HG3-T265S) structure[3], the transition state analog orientation most closely resembling that in HG3.17 was used. In order to model the position of the acidic proton at N1 in the HG2 complex, a calculated structure of 6-nitrobenzotriazole was pair-fitted onto the ligand in the X-ray structure. Ψ is the angle at the acceptor atom; θ, the angle at the hydrogen atom; and *X*, the torsional angle around the C–O^- axis.